

Microwave response of superconducting pnictides: extended s_{\pm} scenario

O.V. Dolgov¹

A.A. Golubov²

D. Parker³

¹Max-Planck-Institut für Festkörperforschung, D-70569 Stuttgart, Germany

²Faculty of Science and Technology and MESA+ Institute of Nanotechnology, University of Twente, 7500 AE Enschede, The Netherlands

³Naval Research Laboratory, 4555 Overlook Ave. SW, Washington, DC 20375

Abstract. We consider a two-band superconductor with the relative phase π between the two order parameters as a model for superconducting state in ferropnictides. Within this model we calculate the microwave response and the NMR relaxation rate. Influence of intra- and interband impurity scattering beyond the Born limit (the resonant scattering) is taken into account. We show that, depending on the scattering rate, various types of power low temperature dependencies of the magnetic field penetration depth and the NMR relaxation rate at low temperatures may take place.

PACS numbers: 74.20.Rp, 76.60.-k, 74.25.Nf, 71.55.-i

1. Introduction

The recent discovery of Fe-based superconducting compounds [1] has stimulated the research of unconventional superconductors. One of the most important and still unsettled issues is the symmetry of superconducting gap function. So far, different experiments produce conflicting results. As regard measurements of the penetration depth and the NMR relaxation rate, a power law behavior at low temperatures is now clearly established, which is a signature of unconventional order parameter symmetry. One possible scenario of a pairing symmetry state is a superconductor consisting of two relatively small semimetallic Fermi surfaces, separated by a finite wave vector \mathbf{Q} with the relative phase π between the two order parameters. This is the so-called s_{\pm} model, first proposed in Ref. [2]. In our previous work [3] we have shown that s_{\pm} model with resonant impurity scattering can explain power law behavior of NMR relaxation rate. Therefore it is important to extend this formalism to address microwave properties of a two-band s_{\pm} superconductor, in particular the magnetic field penetration depth and real part of complex conductivity, since experimental data are now available for high quality single crystals of Fe-based superconducts.

In this paper we calculate microwave response and the NMR relaxation rate for a model s_{\pm} superconductor in which impurity scattering is treated beyond the Born limit and discuss the relevance to experimental data for Fe-based superconducting compounds.

2. General expressions

We describe a multiband superconductor in the framework of the Eliashberg approach equations for the renormalization function $Z_i(\omega)$ and complex order parameter $\phi_i(\omega)$. On the real frequency axis they have the following form, assuming an *uniform* (band-independent) impurity scattering (see e.g., Ref.[3, 4, 5])

$$\begin{aligned}\phi_i(\omega) &= \sum_j \int_{-\infty}^{\infty} dz K_{ij}^{\Delta}(z, \omega) \text{Reg}_j^{\Delta}(z) + i \frac{\gamma}{2\mathcal{D}} (g_1^{\Delta}(\omega) - g_2^{\Delta}(\omega)) \\ (Z_i(\omega) - 1)\omega &= \sum_j \int_{-\infty}^{\infty} dz K_{ij}^Z(z, \omega) \text{Reg}_j^Z(z) + i \frac{\gamma}{2\mathcal{D}} (g_1^Z(\omega) + g_2^Z(\omega)),\end{aligned}\quad (1)$$

where $\mathcal{D} = 1 - \sigma + \sigma \left[(g_1^Z(\omega) + g_2^Z(\omega))^2 + (g_1^{\Delta}(\omega) - g_2^{\Delta}(\omega))^2 \right]$. For our model $g_i^Z(\omega) = n_i(\omega) Z_i(\omega) \omega / D_i(\omega)$, $g_i^{\Delta}(\omega) = n_i(\omega) \phi_i(\omega) / D_i(\omega)$, where $D_j(\omega) = \sqrt{[Z_j(\omega)\omega]^2 - \phi_j^2(\omega)}$ and $n_i(\omega)$ is a partial density of states. $\gamma = \frac{c\pi N(0)v^2}{1 + [\pi N(0)v]}$ is the normal state scattering rate and $\sigma = \frac{[\pi N(0)v]^2}{1 + [\pi N(0)v]^2}$ is the impurity strength ($\sigma \rightarrow 0$ corresponds to the Born limit, while $\sigma = 1$ to the unitary one). Kernels $K_{ij}^{\Delta, Z}(z, \omega)$ describe *electron-boson interaction* and have forms

$$K_{ij}^{\Delta, Z}(z, \omega) = \int_0^{\infty} d\Omega \frac{\tilde{B}_{ij}(\Omega)}{2} \left[\frac{\tanh \frac{z}{2T} + \coth \frac{\Omega}{2T}}{z + \Omega - \omega - i\delta} - \{\Omega \rightarrow -\Omega\} \right],$$

where $\tilde{B}_{ij}(\Omega) = B_{ij}(\Omega)$ for the equation for Δ , and $|B_{ij}(\Omega)|$ for the equation for Z . Note that all retarded interactions enter the equations for the renormalization factor Z with a positive sign.

The microwave conductivity in the London (local, $\mathbf{q} \equiv 0$) limit is given by

$$\sigma^i(\omega) = \omega_{pl,i}^2 \Pi_i(\omega) / 4\pi i \omega, \quad (2)$$

where $\Pi_i(\omega)$ is an analytical continuation to the real frequency axis of the polarization operator (see, e.g. Refs. [6],[7],[8],[9],[10])

$$\begin{aligned} \Pi_i(\omega) &= \left\{ i\pi T \sum_n \Pi_i(\omega_n, \nu_m) \right\}_{i\omega_m \Rightarrow \omega + i0^+}, \\ \Pi_i(\omega) &= \int d\omega' \left\{ \frac{\tanh\left(\frac{\omega_-}{2T}\right)}{D^R} \left[1 - \frac{\tilde{\omega}_-^R \tilde{\omega}_+^R + \phi_-^R \phi_+^R}{\sqrt{(\tilde{\omega}_-^R)^2 - (\phi_-^R)^2} \sqrt{(\tilde{\omega}_+^R)^2 - (\phi_+^R)^2}} \right] - \right. \\ &\quad \frac{\tanh\left(\frac{\omega_+}{2T}\right)}{D^A} \left[1 - \frac{\tilde{\omega}_-^A \tilde{\omega}_+^A + \phi_-^A \phi_+^A}{\sqrt{(\tilde{\omega}_-^A)^2 - (\phi_-^A)^2} \sqrt{(\tilde{\omega}_+^A)^2 - (\phi_+^A)^2}} \right] - \\ &\quad \left. \frac{\tanh\left(\frac{\omega_{\pm}}{2T}\right) - \tanh\left(\frac{\omega}{2T}\right)}{D^a} \left[1 - \frac{\tilde{\omega}_-^A \tilde{\omega}_+^R + \phi_-^A \phi_+^R}{\sqrt{(\tilde{\omega}_-^A)^2 - (\phi_-^A)^2} \sqrt{(\tilde{\omega}_+^R)^2 - (\phi_+^R)^2}} \right] \right\}, \end{aligned} \quad (3)$$

where

$$D^{R,A} = \sqrt{(\tilde{\omega}_+^{R,A})^2 - (\phi_+^{R,A})^2} + \sqrt{(\tilde{\omega}_-^{R,A})^2 - (\phi_-^{R,A})^2},$$

and

$$D^a = \sqrt{(\tilde{\omega}_+^R)^2 - (\phi_+^R)^2} - \sqrt{(\tilde{\omega}_-^A)^2 - (\phi_-^A)^2},$$

$\omega_{\pm} = \omega' \pm \omega/2$, and the index $R(A)$ corresponds to the retarded (advanced) brunch of the complex function $F^{R(A)} = ReF \pm iImF$ (the band index i is omitted). Here $\omega_{pl}^{\alpha\beta} = \sqrt{8\pi e^2 \langle N_i(0) v_F^{\alpha} v_F^{\beta} \rangle}$ is the plasma frequency in different directions. For dirty *intra-band-impurity* case the low frequency limits of expressions 2 and 3 can be reduced to

$$\begin{aligned} \sigma_1(\omega \rightarrow 0) &= \sigma_1^{\text{dc}} \int_0^{\infty} d\omega \left(-\frac{\partial f(\omega)}{\partial \omega} \right) \left\{ [\text{Reg}_1^Z(\omega)]^2 + [\text{Reg}_1^A(\omega)]^2 \right\} + \\ &\quad \sigma_2^{\text{dc}} \int_0^{\infty} d\omega \left(-\frac{\partial f(\omega)}{\partial \omega} \right) \left\{ [\text{Reg}_2^Z(\omega)]^2 + [\text{Reg}_2^A(\omega)]^2 \right\}, \end{aligned} \quad (4)$$

where $\sigma_i^{\text{dc}} = v_F^2 e^2 \tau_i$ is a contribution to the static conductivity from i -th band. Note that in the London limit there are no *cross-terms* connected two bands.

An important characteristic of the superconducting state is **the penetration depth** of the magnetic field $\lambda_{L,\alpha\beta}$ in the local (London) limit, which is related to the imaginary part of the optical conductivity by

$$1/\lambda_{L,\alpha\beta}^2 = \lim_{\omega \rightarrow 0} 4\pi\omega \text{Im} \sigma^{\alpha\beta}(\omega, \mathbf{q} = 0) / c^2 \equiv \omega_{pl,i}^{\alpha\beta 2} \text{Re} \Pi_i(\omega = 0) / c^2, \quad (5)$$

where α, β denote again Cartesian coordinates and c is the velocity of light. If we neglect strong-coupling effects (or, more generally, Fermi-liquid effects) then for a clean uniform superconductor at $T = 0$ we have the relation $\lambda_{L,\alpha\beta} = c/\omega_{pl}^{\alpha\beta}$. Impurities and interaction effects drastically enhance the penetration depth, and it is suitable to introduce a so called 'superfluid plasma frequency' $\omega_{pl,\alpha\beta}^{sf}$ by the relation $\omega_{pl,\alpha\beta}^{sf} = c/\lambda_{L,\alpha\beta}$. It has been often mentioned that this function corresponds to the charge density of the superfluid condensate, but we would like to point out that this is only the case for noninteracting clean systems at $T = 0$.

In the two-band model we have the standard expression (neglecting vertex corrections)

$$1/\lambda_{L,\alpha\beta}^2(T) \equiv (\omega_{pl,\alpha\beta}^{sf}(T)/c)^2 = \sum_i \left(\frac{\omega_{pl,i}^{\alpha\beta}}{c} \right)^2 \pi T \sum_{n=-\infty}^{\infty} \frac{\tilde{\Delta}_i^2(n)}{[\tilde{\omega}_i^2(n) + \tilde{\Delta}_i^2(n)]^{3/2}}, \quad (6)$$

where $\tilde{\omega}(n)$ and $\tilde{\Delta}(n)$ are the solutions of Eq. 1 continued to the imaginary (Matsubara) frequencies ($\tilde{\Delta}_i(n) = \phi_i(i\omega_n)$, $\tilde{\omega}_i(n) = \omega_n Z_i(i\omega_n)$). The calculations along these formulas can be thus presented in form of the effective superfluid plasma frequency, ω_{pl}^{sf} .

For **the NMR relaxation rate**, following Samokhin and Mitrović [11], we can write down the following general expressions.

$$1/T_1 T = -\frac{1}{2\pi} \lim_{\omega \rightarrow 0} \sum_{\mathbf{q}} [F(\mathbf{q})]^2 \frac{Im\chi_{\pm}(\mathbf{q}, \omega)}{\omega}, \quad (7)$$

where $\chi_{\pm}(\mathbf{q}, \omega)$ is an analytical continuation to the real axis of the Fourier transform of the correlator

$$\chi_{\pm}(\mathbf{r}, \tau) = -\langle\langle T_{\tau}(S_{+}(\mathbf{r}, -i\tau)S_{-}(\mathbf{0}, 0)) \rangle\rangle_{imp}.$$

averaged over impurity ensemble. Here $S_{\pm}(\mathbf{r}, -i\tau) = \exp(H\tau)S_{\pm}(\mathbf{r})\exp(-H\tau)$ where H is the electron Hamiltonian, τ denotes imaginary time, and $S_{+}(\mathbf{r}) = \psi_{\uparrow}^{\dagger}(\mathbf{r})\psi_{\downarrow}(\mathbf{r})$ and $S_{-}(\mathbf{r}) = \psi_{\downarrow}^{\dagger}(\mathbf{r})\psi_{\uparrow}(\mathbf{r})$. As a result we have

$$1/T_1 T = \frac{1}{\pi^2} \sum_{\mathbf{k}_1, \mathbf{k}_2} \int_{-\infty}^{\infty} d\omega \left(-\frac{\partial f(\omega)}{\partial \omega} \right) \sum_{i,j} [F_{ij}(\mathbf{k}_1 - \mathbf{k}_2)]^2 \times \left[Im \frac{\omega Z_{i,\mathbf{k}_1}(\omega)}{D_{i,\mathbf{k}_1}(\omega)} Im \frac{\omega Z_{j,\mathbf{k}_2}(\omega)}{D_{j,\mathbf{k}_2}(\omega)} + Im \frac{\xi_{i,\mathbf{k}_1}}{D_{i,\mathbf{k}_1}(\omega)} Im \frac{\xi_{j,\mathbf{k}_2}}{D_{j,\mathbf{k}_2}(\omega)} + Im \frac{\phi_{i,\mathbf{k}_1}(\omega)}{D_{i,\mathbf{k}_1}(\omega)} Im \frac{\phi_{j,\mathbf{k}_2}(\omega)}{D_{j,\mathbf{k}_2}(\omega)} \right]. \quad (8)$$

Here $D_{i,\mathbf{k}_1}(\omega) = [\omega Z_{i,\mathbf{k}_1}(\omega)]^2 - \xi_{i,\mathbf{k}_1}^2 - \phi_{i,\mathbf{k}_1}^2(\omega)$, ξ_{i,\mathbf{k}_1} is the bare energy. For the Fermi-contact interaction

$$\frac{1}{T_1 T} \propto \int_0^{\infty} d\omega \left(-\frac{\partial f(\omega)}{\partial \omega} \right) \left\{ [\text{Reg}_1^Z(\omega) + \text{Reg}_2^Z(\omega)]^2 + [\text{Reg}_1^{\Delta}(\omega) + \text{Reg}_2^{\Delta}(\omega)]^2 \right\}. \quad (9)$$

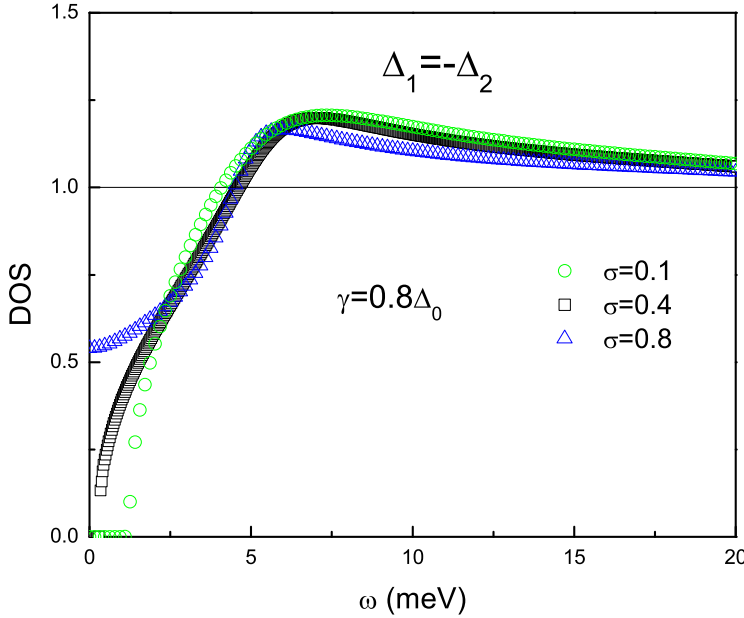


Figure 1. (color online) The quasiparticle density-of-states for the three indicated cases.

The above formula has been used in Ref.[3]. This expression contains *the cross-term* in contrast to the microwave conductivity. For a single band system it is proportional to Eq.4 when $\sigma_1^{\text{dc}} \rightarrow \infty$ (Ref. [12]), but, in principle, in multiband systems and for finite intraband impurity scattering $1/T_1 T$ and $\sigma_1(\omega \rightarrow 0)$ can behave differently.

3. Results and discussion

It is well known that pair-breaking impurity scattering can induce substantial sub-gap density-of-states, which can produce power-law low temperature behavior in a whole host of thermodynamic quantities, such as specific heat, London penetration depth, nuclear spin relaxation rate, and even optical conductivity. Such behavior has been well-studied in the two canonical limits of weak (Born) scattering and strong (unitary) scattering [13], but the intermediate regime has received almost no attention. In addition, with the advent of the multiband superconductivity in MgB_2 and the apparent multiband, *primarily interband* superconductivity in the pnictides, comes a need for further study of the intermediate regime in an interband case. Recent studies [14, 15] have addressed the effects of impurities in the pnictides, but only in the Born or unitary limits. Here we study the important and likely more realistic intermediate regime, with σ , effectively the scattering strength (see [3] for a definition), not the conductivity, taken as 0.1, 0.4, and 0.8. Note that the Born limit corresponds to $\sigma \rightarrow 0$ while the unitary limit corresponds to $\sigma = 1$.

We will now illustrate the above discussion using specific numerical models. First, we present numerical solutions of the Eliashberg equations using a spin-fluctuation model for

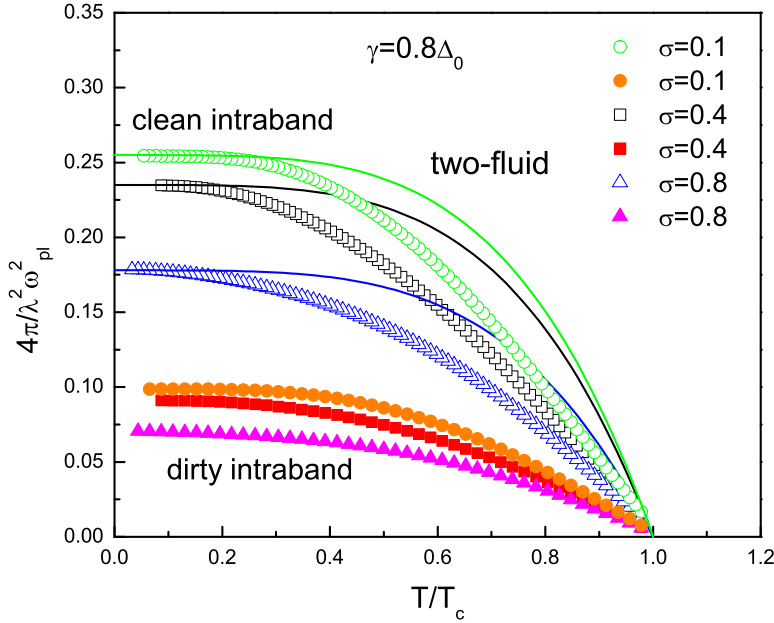


Figure 2. (color online) The inverse squared penetration depth

the spectral function of the intermediate boson: $B_{ij}(\omega) = \lambda_{ij}\pi\omega\Omega_{sf}/(\Omega_{sf}^2 + \omega^2)$, with the parameters $\Omega_{sf} = 25\text{meV}$, $\lambda_{11} = \lambda_{22} = 0.5$, and $\lambda_{12} = \lambda_{21} = -2$. This set gives a reasonable value for $T_c \simeq 26.7\text{K}$. A similar model was used in Ref. [16] to describe optical properties of ferropnictides. This model was also used in [3] and for consistency is used here. We further assume that each surface features the same gap [17].

We begin with the density-of-states, shown below in Figure 1. As in [3], we have chosen a relatively large impurity scattering ($\Gamma = 0.8\Delta_0$), which is to be expected considering the early state of pnictide sample preparation and the limited availability of large single crystals. Several effects are apparent. Firstly, for all three σ values the substantial peak usually present at $\omega = \Delta_0$ (about 6 meV here) is substantially truncated, with much spectral weight transferred below the gap. However, the detailed sub-gap behavior depends radically upon the scattering strength σ . The near-Born case $\sigma = 0.1$ still retains a small minigap of approximately 1.5 meV, which will lead to exponentially activated behavior below about 4 Kelvin. Although some data has shown evidence for such exponentially activated behavior, there is also significant data showing power-law behavior. The intermediate case $\sigma = 0.4$ shows a monotonically increasing density of-states and essentially no minigap, leading to power-law behavior, as proposed in [3]. Finally, the near-unitary case $\sigma = 0.8$ also shows a monotonically increasing density-of-states, but is nearly constant at low energy. We will see that such behavior leads to a quadratic temperature dependence of the penetration depth, even without the assumption of the strict unitary limit. We note parenthetically that the behavior depicted depends rather strongly upon the large value of impurity scattering assumed; the first two cases will yield

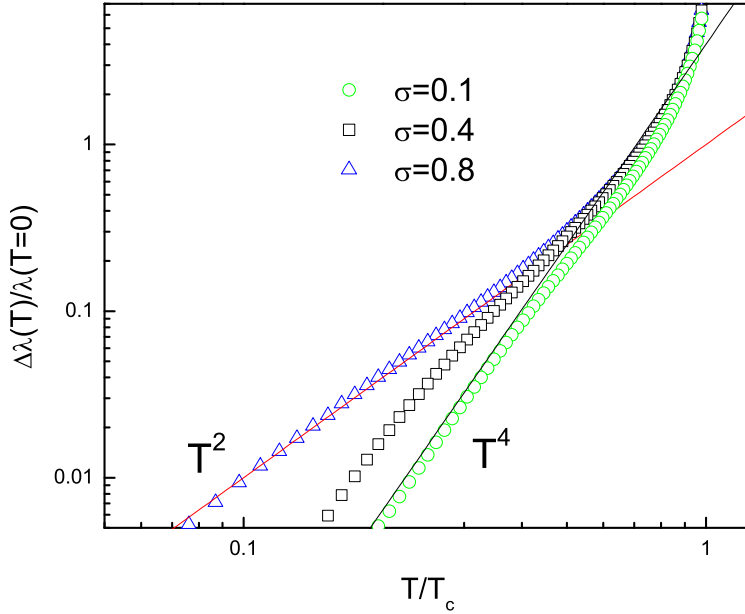


Figure 3. (color online) Low temperature behavior of the penetration depth

more exponentially activated behavior if the scattering rate is much less strong, while the near-unitary case can potentially [4] lead to a non-monotonic density of states.

The London penetration depth has been calculated for two sets of parameters: a) clean intraband $\gamma_{11} = \gamma_{22} = 0$, and b) dirty intraband $\gamma_{11} = \gamma_{22} = 300\text{cm}^{-1} \gg \Delta$. In both cases the temperature dependence of the inverted squared penetration depth (or so called superfluid density) is different from the standard two-fluid (Gorter-Kazimir) model $\lambda^{-2}(T) = \lambda^{-2}(0) \left[1 - (T/T_c)^4\right]$, that is similar to the BCS result. In Figure 2 is shown the inverse squared London penetration depth $1/\lambda^2(T)$ for several cases. The top three cases refer to a scenario in which the intraband impurity scattering has been taken to be zero, but the interband scattering has the indicated value, while the lower three contain an extremely large impurity scattering $\sim 10\Delta_0$. As is to be expected, the clear intraband $\sigma = 0.1$ case shows an exponentially activated behavior at low temperature, while the intermediate and near-unitary cases clearly show power-law behavior, with the actual power varying between 1 and 2.

Regarding the dirty intraband limit, we note that Anderson's theorem, in which intraband scattering does not substantially affect superconducting properties, is at work here, but that in this case this theorem only applies in the *intraband* channel. Due to the sign change between gaps, *interband* scattering is strongly pair-breaking, analogously to magnetic scattering in s-wave superconductors. The near-Born case retains its near-exponential character at low T, while the other two cases again approach power law behavior.

A more detailed view of the low-temperature $\lambda(T)$ power law behavior is presented in Figure 3, which shows $\Delta\lambda(T)/\lambda_{T=0}$ for the same three cases. We see that the near-Born limit

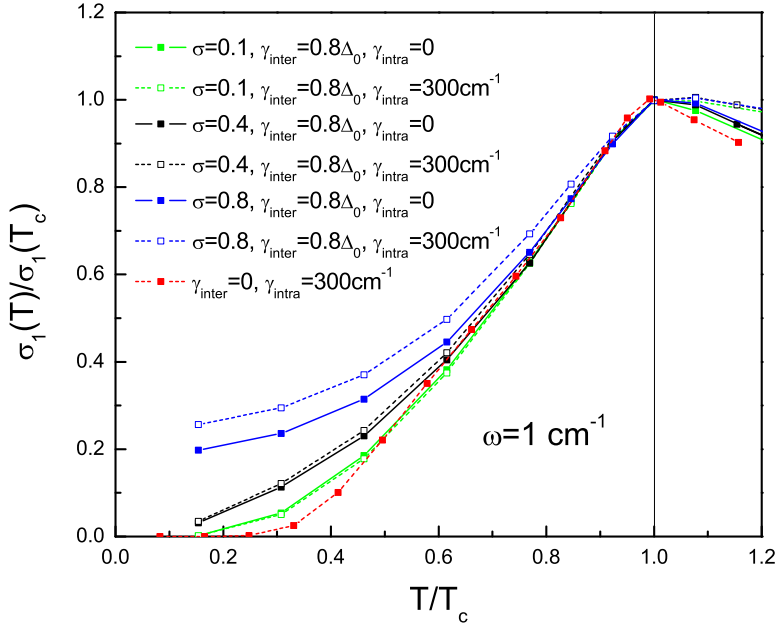


Figure 4. (color online) The real part of microwave conductivity

case ($\sigma = 0.1$) approaches a T^4 behavior, reminiscent of a two fluid model, while the near-unitary case shows a fairly robust T^2 behavior and the intermediate case falls between these two limits, as one would naively expect. Experimental data available so far [19, 20, 21] are consistent either by T^2 either T^4 or exponential (gapped) behavior. Within our model, both results can be explained by proper choice of the impurity scattering rate. It is interesting to note that the T^2 dependence we obtain corresponds to strongly gapless regime. Similar results were obtained recently in Ref.[15] but in the Born limit only.

Figure 4 shows the calculated real part of the microwave conductivity for the three cases above, with two levels of intraband impurity scattering, as indicated, as well as a case in which the interband scattering is entirely neglected. The microwave conductivity (Fig. 4) $\sigma_1(T)$ does not show the coherence peak near T_c . The suppression is connected with strong-coupling effects (see, [18]). Below T_c the behavior of the $\sigma_1(T)$ is determined by the filling of the impurity induced states below Δ . Qualitatively it is similar to the temperature dependence of the NMR relaxation rate (see Fig. 5), but in the latter case the Hebel-Slichter peak is additionally reduced for s_{\pm} model by the different kind of the coherence factor. The plot makes plain the radically different effects of intraband and interband impurity scattering upon the conductivity. The $\gamma_{inter} = 0$ case shows this most clearly; despite the large value of γ_{intra} the conductivity vanishes exponentially at low temperatures, and for the near-Born limit and intermediate case the large intraband scattering has essentially no effect on $\sigma(T)$, with a modest impact only in the near-unitary limit case. Almost all of the non-canonical BCS behavior derives from the interband scattering, which results in near constant behavior

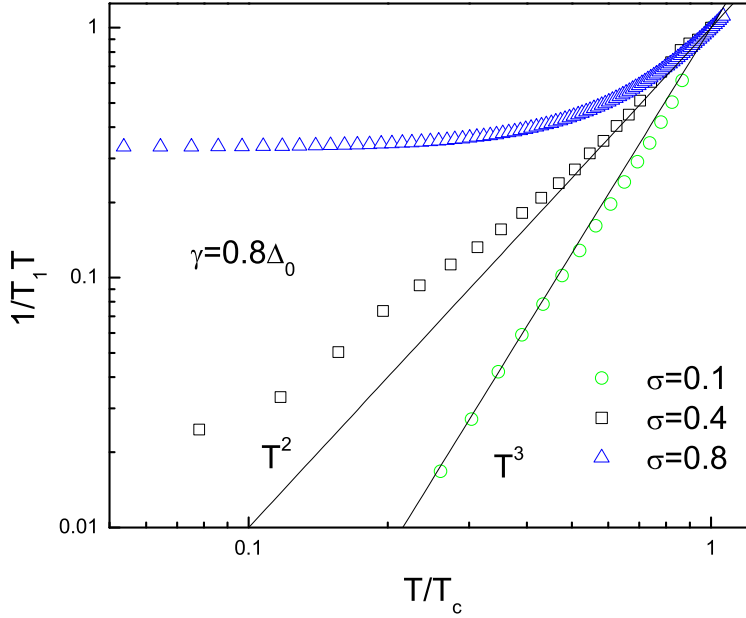


Figure 5. (color online) The temperature dependence the $1/T_1T$

at low T for the near-unitary case, as might be expected from the form of Equation 4, in which a squared density-of-states enters. The intermediate case shows power law behavior as well, with the precise exponent not extracted.

Finally we turn in Figure 5 to the nuclear spin relaxation rate T_1^{-1} for the same three σ scenarios, except that in this case the interband and intraband scattering have been taken equal. Note also that following convention we have plotted $(T_1T)^{-1}$ rather than T_1^{-1} , and all power-law references here mean $(TT_1)^{-1}$. T_1 has been a source of substantial controversy in the pnictides due to the existence of several data-sets [22, 23, 24, 25] showing near- T^2 behavior throughout nearly the entire temperature range, although there now exist data [26] deviating from this behavior. Several things are apparent from the plot: first of all, the near-Born limit case shows power law behavior ($1/T_1T \sim T^3$) throughout nearly the entire temperature range below T_c , although it will ultimately revert to exponentially activated behavior at the lowest temperatures. Substantial impurity scattering in the Born limit can thus mimic much of the behavior commonly ascribed to nodes, as was noted in [15]. The intermediate case shows an approximate $T^{1.5}$ behavior, as was described in [3], which is largely driven by the monotonic density-of-states presented in Figure 1, where the same parameters are chosen. Korringa behavior results in the near-unitary limit, as is again a direct consequence of the corresponding behavior of the density-of-states in Figure 1.

It should now be clear that impurity scattering in various strengths (i.e., σ), if sufficient impurity concentrations are present, can produce a wide variety of power-law behaviors in many thermodynamic quantities, even in the near-Born limit. In the s_{\pm} state, interband

impurities are clearly much more effective in creating such behavior, although as seen in the penetration depth results, extremely large intraband scattering can have an effect as well. This has implications for the ongoing lively debate about pairing symmetry, with significant numbers of proposals for nodal superconductivity in the pnictides and some experimental evidence for such behavior.

In conclusion, we have calculated the microwave response and the NMR relaxation rate for a superconductor in s_{\pm} symmetry state by solving Eliashberg equations with a model spectrum and taking into account impurity scattering beyond the Born limit. We show that the T^2 temperature behavior of the penetration depth and the NMR relaxation rate at low temperatures can be reproduced in this model. We have also demonstrated the dramatic effect of the interband scattering on the real part of the microwave conductivity, which in particular results in near constant behavior at low T for the near-unitary case.

- [1] Y. Kamihara *et al.*, J. Am. Chem. Soc. **130**, 3296 (2008).
- [2] I.I. Mazin, D.J. Singh, M.D. Johannes, and M.H. Du, Phys. Rev. Lett, 101, 057003 (2008).
- [3] D. Parker, O. V. Dolgov, M. M. Korshunov, A.A. Golubov and I.I. Mazin, Phys. Rev. B **78**, 134524 (2008).
- [4] G. Preosti and P. Muzikar, Phys. Rev. B **54**, 3489 (1996).
- [5] A.A. Golubov and I.I. Mazin, Phys. Rev. B **55**, 15146 (1997).
- [6] S.B. Nam, Phys. Rev., **156**, 470 (1967).
- [7] W. Lee, D.Rainer, and W. Zimmermann, Physica C **159**, 535 (1988).
- [8] O.V. Dolgov, A.A. Golubov, and S.V. Shulga, Phys. Letters A **147**, 317 (1990).
- [9] R. Akis and J.P. Carbotte, Solid State Comm., **79**, 577 (1991).
- [10] F. Marsiglio, Phys. Rev. B **44**, 5373 (1991).
- [11] K.V. Samokhin and B. Mitrović, Phys. Rev. B **72**, 134511 (2005); *ibid* **74**, 144510 (2006).
- [12] F. Marsiglio, J.P. Carbotte, R. Akis, D. Achkir, and M. Poirier, Phys Rev. B **50**, 7203(R), (1994).
- [13] P.J. Hirschfeld, P. Wölfle, and D. Enzel, Phys. Rev. B **37**, 83 (1988); A.E. Karakozov, E.G. Maksimov, and A.V. Andrianova, JETP Letters, **79**, 329 (2004).
- [14] Y. Bang, arXiv:0902.1020 (unpublished).
- [15] A.V. Vorontsov, M.G. Vavilov, A.V. Chubukov, arXiv:0901.0719 (unpublished).
- [16] J. Yang, D. Huvonen, U. Nagel, T. Room, N. Ni, P.C. Canfield, S.L. Budko, J.P. Carbotte, and T. Timusk, arXiv:0807.1040 (unpublished).
- [17] In the weak coupling limit, the gap ratio at $T \rightarrow T_c$ in the s_{\pm} model is $\sqrt{N_1/N_2}$, where N_i are densities of states. LDA calculations yield $N_e/N_h < 1.2$, therefore Δ_1 and Δ_2 differ by less than 10%. Strong coupling effects additionally reduce the gaps ratio (see, O.V. Dolgov, I.I. Mazin, D. Parker, and A.A. Golubov, Phys. Rev. B **79**, 060502(R) (2009); O.V. Dolgov and A.A. Golubov, Phys. Rev. B **77**, 214526 (2008)).
- [18] O.V. Dolgov, A.A. Golubov, and A.E. Koshelev, Solid State Comm. **72**, 81 (1989); P.B. Allen and D. Rainer, Nature **439**, 396 (1991).
- [19] C. Martin, M. E. Tillman, H. Kim, M. A. Tanatar, S. K. Kim, A. Kreyssig, R. T. Gordon, M. D. Vannette, S. Nandi, V. G. Kogan, S. L. Bud'ko, P. C. Canfield, A. I. Goldman, and R. Prozorov, arXiv:0903.2220 (unpublished); C. Martin, R.T. Gordon, M. A. Tanatar, H. Kim, N. Ni, S. L. Bud'ko, P. C. Canfield, H. Luo, H. H. Wen, Z. Wang, A. B. Vorontsov, V. G. Kogan, and R. Prozorov, arXiv:0902.1804 (unpublished); R. T. Gordon, C. Martin, H. Kim, N. Ni, M. A. Tanatar, J. Schmalian, I. I. Mazin, S. L. Bud'ko, P. C. Canfield, and R. Prozorov, arXiv:0812.3683 (unpublished).
- [20] L. Malone, J.D. Fletcher, A. Serafin, A. Carrington, N.D. Zhigadlo, Z. Bukowski, S. Katrych, and J. Karpinski, arXiv:0806.3908 (unpublished).
- [21] K. Hashimoto, T. Shibauchi, S. Kasahara, K. Ikada, T. Kato, R. Okazaki, C. J. van der Beek, M. Konczykowski, H. Takeya, K. Hirata, T. Terashima, and Y. Matsuda, arXiv:0810.3506 (unpublished);

- K. Hashimoto, T. Shibauchi, T. Kato, K. Ikada, R. Okazaki, H. Shishido, M. Ishikado, H. Kito, A. Iyo, H. Eisaki, S. Shamoto, and Y. Matsuda, *Phys. Rev. Lett.* **102**, 017002 (2009).
- [22] H.-J. Grafe, D. Paar, G. Lang, N.J. Curro, G. Behr, J. Werner, J. Hamann-Borrero, C. Hess, N. Leps, R. Klingeler, and B. Büchner, *Phys. Rev. Lett.* **101**, 047003 (2008).
- [23] Y. Nakai, K. Ishida, Y. Kamihara, M. Hirano, and H. Hosono, *Phys. Rev. Lett.* **101**, 077006 (2008).
- [24] K. Matano, Z.A. Ren, X.L. Dong, L.L. Sun, Z.X. Ghao, and G.-Q. Zheng, *Europhys. Lett.* **83**, 57001 (2008).
- [25] H. Mukuda, N. Terasaki, H. Kinouchi, M. Yashima, Y. Kitaoka, S. Suzuki, S. Miyasaka, S. Tajima, K. Miyazawa, P.M. Shirage, H. Kito, H. Eisaki, and A. Iyo, *J. Phys. Soc. Jpn.* **77**, 093704 (2008); H. Kotegawa, S. Masaki, Y. Awai, H. Tou, Y. Mizuguchi and Y. Takano, *J. Phys. Soc. Jpn.* **77**, 113703 (2008).
- [26] Y. Kobayashi, A. Kawabata, S.C. Lee, T. Moyoshi and M. Sato, arXiv:0901.2830 (unpublished); H. Fukazawa, T. Yamazaki, K. Kondo, Y. Kohori, N. Takeshita, P.M. Shirage, K. Kihou, K. Miyazawa, H. Kito, H. Eisaki, and A. Iyo, arXiv:0901.0177 (unpublished); K. Tatsumi, N. Fujiwara, H. Okada, H. Takahashi, Y. Kamihara, M. Hirano, and H. Hosono, *Journal of Phys. Soc. Jpn.*, **78**, 023709 (2009).